Surface modified polythiophene nanocomposite using HPC and DBSNa for heavy metal ion removal

Vahideh Arabahmadi and Mohsen Ghorbani

ABSTRACT

In the present work, surface modified nanocomposite adsorbents polythiophene (PTh)/rice husk ash (RHA) have successfully been synthesized in the presence of hydroxyl propyl cellulose (HPC) and sodium dodecyl benzene sulfonate (DBSNa) as surfactants. The synthesized nanoparticles were characterized by scanning electron microscopy (SEM), transmission electron microscopy (TEM) and Fourier transform infrared spectroscopy (FTIR), and the synthesized nanocomposite adsorbents were applied as an efficient sorbent for Pb(II) ion removal from contaminated water and the removal efficiency was compared to pure PTh/RHA composite. Several variables affecting the extraction efficiency of the nanoadsorbent i.e., adsorbent dosage, metal ion concentration, extraction time, and adsorption conditions were investigated. The highest efficiency of adsorption (98.12%) was achieved with 0.05 g of PTh/RHA/HPC nanocomposite adsorbent in 50 mL of 10 mg/L Pb(II) solution. Equilibrium studies were also performed with known linear and non-linear adsorption isotherms including Langmuir, Freundlich and Sips from which the best result was achieved with Freundlich and Sips isotherms representing multilayer adsorption on heterogeneous structure of the adsorbent. The pseudo-first-order model and the pseudo-second-order model were adopted to analyze the adsorption kinetics of Pb(II) on PTh/RHA/HPC and PTh/RHA/DBSNa. The consistency of the experimental adsorption capacity with the ones calculated from the pseudo-second-order kinetic model illustrated that the adsorption of Pb(II) onto both adsorbents at initial concentration of 50 mg/L was probably controlled by chemical adsorption.

Key words | DBSNa, HPC, lead ion adsorption, polythiophene, rice husk ash

Vahideh Arabahmadi
Shomal University,
P.O. Box 731,
Amol,
Iran

Mohsen Ghorbani (corresponding author)
Department of Chemical Engineering,
Babol Noshirvani University of Technology,
Shariati Ave.,
Babol 47148-71167,
Iran
E-mail: *m.ghorbani@nit.ac.ir*

INTRODUCTION

Lead (Pb(II)) is one of the most toxic and carcinogenic heavy metals and has detrimental effects on the environment and human health (Bradl 2005). Pb(II) ions enter into water sources from mining, metallurgical processes, metal plating and gasoline industries, which can impose side effects on human blood circulation and nervous system, kidneys, and reproductive system, even at small concentrations of 15 μg/L (Yaşar *et al.* 2011; Vatani & Eisazadeh 2013). Many efforts have been performed to remove these toxic heavy metals from water sources in order to provide high quality water. In this regards, processes including membrane filtration, ion exchange, electrocatalytic separation and adsorption were applied (Barakat 2011; Lee *et al.* 2011). However, among all methods, adsorption gained much attention from environmentalists due to simplicity, good quality and lower costs (Ali & Gupta 2006; Ren *et al.* 2011). Several materials have been applied as adsorbents; for instance, carbon nanotubes, zeolites, biopolymers, modified nano-sized adsorbents and dendrimers (Theron *et al.* 2008; Miretzky & Cirelli 2009). In a wide range of applications, conductive polymers including polyaniline, polyacetylene, polypyrrole, and polythiophene (PTh) have attracted the researchers all over the world to be used as rechargeable batteries (Li *et al.* 1992), electromagnetic interference shielding (MacDiarmid & Epstein 1995), antistatic coatings (Ohtani *et al.* 1993), gas sensors (Matsuguchi *et al.* 2002), optical devices (Falcão & de Azevêdo 2002) and removal of heavy metals (Eisazadeh 2007; Ghorbani *et al.* 2010).

In recent years, PTh has attracted much attention in many scientific studies due to chemical stability in

doi: 10.2166/wst.2017.140

air/humid environments. A noticeable point in application of conductive polymers is their processability, which provides best efficiency when composite materials are generated using these polymers as the base matrix (Ghorbani & Eisazadeh 2012). On the other hand, natural lignocellulosic fibers are gaining attention as filler phase in polymer matrices. Low density, reduced processing machinery wearing, and their reactive surface could be mentioned as attractive points, together with their abundance and low price. In fact, natural nanoparticles and especially particles from natural waste materials are very interesting to use in polymer composites. Silica nanoparticles mostly achieved from rice husk, rice straw, sugarcane bagasse etc. are much investigated for adsorption purposes. In other words, using these particles in polymer blends and composites is very conventional and it can add some new properties to the polymer matrix.

Xiang Li *et al.* has studied PTh as a fiber coating for solid-phase microextraction (Li *et al.* 2008) and Ansari *et al.* used PTh–sawdust nano-biocomposite for basic dye removal (Ansari *et al.* 2013). However, to the best of our knowledge, there are no publications on application of modified PTh/rice husk ash (RHA) with hydroxyl propyl cellulose (HPC) and dodecyl benzene sulfonate (DBSNa) nanocomposite as sorbents for heavy metal ion removal.

In the present study, PTh was used as the base matrix and RHA was added to the matrix during the polymerization process. Surface modification of rice husk was employed in order to obtain a mesoporous structure for rice husk and increasing of specific surface area. It could also enhance the adsorption efficiency of Pb(II) heavy metal ion from aqueous solution. The resulting adsorbents were analyzed properly and adsorption experiments were carried out to compare and prove the applicability of the sorbents.

MATERIALS AND METHODS

Materials

Thiophene monomer and ferric chloride ($FeCl_3$) were purchased from Merck (Germany) and used as received. Rice husk was procured from local mill at Savadkooh region (Iran). Hydrogen peroxide and lead nitrate, HPC and sodium DBSNa all were purchased from Merck (Germany) and used as received without further purification. Deionized water was used throughout this investigation and thiophene monomers were purified using distillation.

Preparation of RHA

Rice husk was used after washing with distilled water and drying in an oven at about 60°C for 2 h. After washing with acetone and sodium hydroxide (0.3 M) to remove contaminants and drying in oven at about 60°C for 4 h, rice husk was heated up to 500°C for 5 h in a furnace (Thermolyne 48000, USA) at heating rate of approximately 25–30°C/min, to obtain RHA.

Synthesis of surface modified PTh/RHA nanocomposite

For preparation of surface modified PTh/RHA nanocomposite, 3 g $FeCl_3$ was added to 30 mL of water and then uniform solution was achieved using magnetic mixer for 15 min. Then, $FeCl_3$ solution, 0.2 g of RHA and 0.1 g of surfactant (HPC or DBSNa) were dissolved in 20 mL distilled water and added to the solution of 2 mL thiophene as monomer. 5 mL of hydrogen peroxide was added to the solution as catalyst and the reaction was carried out for 5 h at room temperature. The product was then centrifuged and washed several times with distilled water to remove impurities. Finally, it was dried at temperature of about 60°C in oven for 24 h.

Characterization

Fourier transform infrared spectrometer (Shimadzu model 4100, Japan) was employed with a resolution of 4/cm (averaging 50 scans) for determination of functional groups. Scanning electron microscope (Philips model XL30, The Netherlands) operating at an accelerating voltage of 26 kV equipped with energy-dispersive X-ray spectrometer (EDS) was used for determination of adsorbents' morphology. Transmission electron microscopy (TEM) was performed using a transmission electron microscope JEOL 200CX operating at 300 kV. Atomic absorption spectrometer (model 929, Unicam) was used to analyze the concentrations of heavy metal ions. Concentrations were determined using calibration of the instrument in the concentration range of 0.5–10 mg/L.

Adsorption study

Completely mixed batch reactor technique was used to remove lead ions from waste water. Solution of Pb(II)

ions was prepared by dissolving $Pb(NO_3)_2$ salt and the desired concentrations were obtained by diluting the parent solution. Adsorption experiments were performed by agitating 0.1 g of sorbent with 10 mL of 50 mg/L Pb(II) standard solution at room temperature in a shaker with rotating speed of 300 rpm. At the end of adsorption experiment, the sorbate was filtered and the concentration of heavy metals was determined. All experiments were carried out three times with the standard deviation remaining less than 3% for triplicate experiments.

The adsorption capacity of the sorbent was calculated using Equation (1):

$$q_t = \frac{C_0 V_0 - C_t V_t}{m} \quad (1)$$

where q_t is the adsorbent capacity at time t (mg/g), C_0 is the initial concentration of heavy metal ion in the solution (mg/L), V_0 is the initial volume of the solution (L), C_t is the concentration of ion at time t, V_t is the volume of solution at time t and m is the sorbent mass (g).

The equilibrium adsorption capacity of the sorbent can be calculated by inserting the equilibrium values in Equation (1).

In order to investigate the effect of different parameters on the adsorption of Pb(II) ion with the prepared adsorbents, pH, initial concentration, adsorbent amount, time and temperature were varied under batch standard tests using the following procedure:

Effect of pH

To study the effect of pH on adsorption capacity, sodium hydroxide and nitric acid were used to adjust the pH of Pb(II) solutions (50 mg/L) at pH 2, 3, 4, 5 and 6. Then 0.1 g of adsorbent was added to 10 mL of Pb(II) solution and shaken for 2 h at room temperature (25°C) (Srivastava *et al*. 2006). Finally, the sorbate was filtered using Whatman 42, 125 mm filter papers and the concentration of heavy metals was determined.

Equilibrium experiments

Adsorption isotherms were obtained by varying the initial Pb(II) concentration from 50 mg/L to 400 mg/L with 0.1 g of adsorbent in 10 mL solutions with shaking time of 2 h at 25 °C. The percentage removal of lead was expressed as:

$$\text{Pb(II) percentage removal} = \frac{(C_e - C_0)}{C_0} \times 100 \quad (2)$$

where *Ce* is the concentration of ion at equilibrium

Batch kinetic experiments

The effect of agitation time on Pb(II) removal was investigated by adding 0.1 g of adsorbents into 10 mL solution of 50 mg/L Pb(II) concentration in a 50 mL conical glass beaker with mixing times of 5, 10, 15, 30, 45, 60, 120 and 240 min at 25°C.

Thermodynamic studies

The temperature of 50 mg/L Pb(II) solution was changed (25, 35, 45, 55 and 65°C) during adsorption experiments (for the optimum experimental conditions including pH, contact time and adsorbent dosage) to study the thermodynamics of lead ion adsorption on adsorbents. At the end of adsorption experiment, the sorbate was filtered and the concentration of heavy metals was determined.

The original concepts of thermodynamics assume that the change in the entropy is the driving force in an isolated system (energy cannot be gained or lost in an isolated system) (Ho 2003). The heat of adsorption of the adsorbents, ΔH^0 (kJ/mol), the free energy change, ΔG^0 (kJ/mol) and entropy change, ΔS^0 (kJ/mol K) for the adsorption process can be calculated by fitting the Langmuir constant, K_L, to the van 't Hoff equation (Khambhaty *et al*. 2009).

$$LnK_L = \frac{\Delta S^0}{R} - \frac{\Delta H^0}{RT} \quad (3)$$

$$\Delta G^0 = -RT \ln K_L \quad (4)$$

where T is the absolute temperature (K) and R is the universal gas constant (8.314 J/mol K).

RESULTS AND DISCUSSION

Characterization of adsorbents

Morphological characterization of PTh was carried out via scanning electron microscopy (SEM) and TEM methods. Figure 1 illustrates SEM micrographs of RHA, PTh/RHA

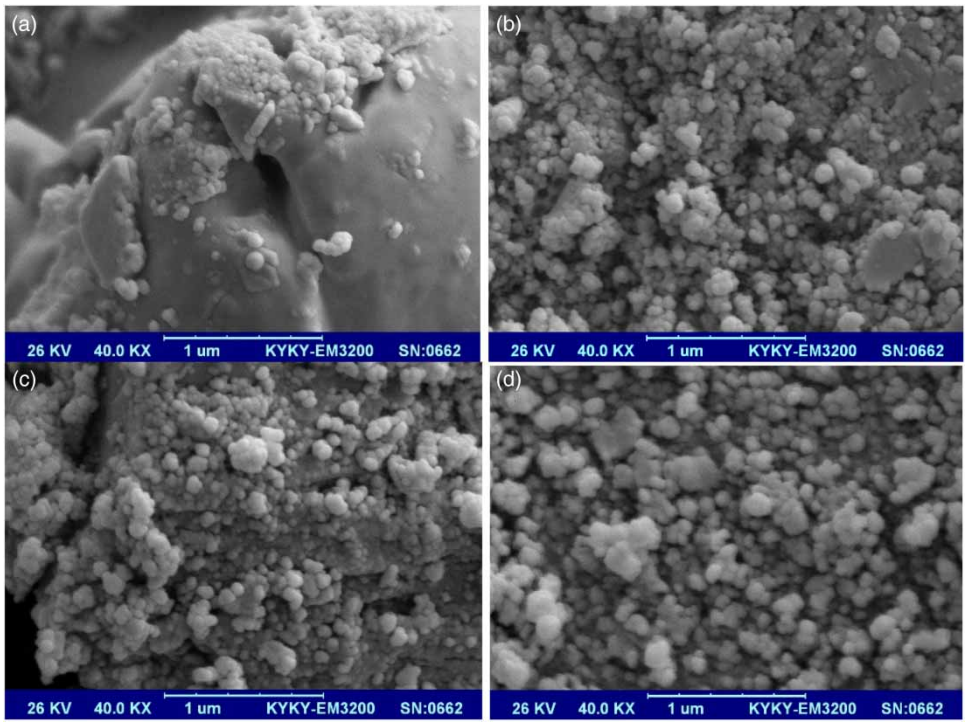

Figure 1 | SEM micrographs of (a) RHA structure, (b) PTh/RHA, (c) PTh/RHA/HPC and (d) PTh/RHA/DBSNa nanocomposite.

and PTh/RHA nanocomposite modified with HPC and DBSNa. The porous structure of RHA with micrometric pores and also complete coating of RHA with PTh is clearly observable. This means that the reaction mixture diffuses into the particles and therefore all the RHA inside and outside the particles is coated with the polymer. However, the porous structure and the coatings can be further confirmed with TEM analysis. The effect of PTh surface modification is also clear in the images and the results have good correlation with SEM images of pure PTh modified samples. Surface modification makes particles smaller and more uniform due to the fact that it causes the neutralization of charged particles by covering their surfaces, which ultimately prevents agglomeration (Rosthauser *et al*. 1991; Dylla-Spears *et al*. 2015). From the results, addition of surfactants leads to the formation of small and uniform particles.

TEM was used to determine nano-sized PTh particles which completely coated RHA. Figure 2 shows the TEM image of PTh/RHA nanocomposite. The presence of black spots determines how deep PTh nanoparticles penetrated into RHA matrix without any aggregation. The uniform dispersion of particles is due to presence of HPC and DBSNa that modified the surface of particles and sorted them together in a uniform manner. The average particle size of PTh nanocomposite particles is 65–85 nm.

Chemical structure of the obtained products was determined by Fourier transform infrared spectroscopy (FTIR), which can prove material interactions in the provided samples. Figure 3 shows the FTIR results for RHA, PTh/RHA and surface modified PTh/RHA with HPC and DBSNa. The details of the observed wavenumbers are completely shown in Table 1, according to which, C-S-C ring deformation absorbance peak, C-H out of plane and in plane deformation, C-S bond stretching, C=C ring stretching and vibration, C-H alkene and aromatic stretching vibrations and adsorbed water in KBr were all observed in the FTIR spectra of the samples (Liu & Liu 2009; Xu *et al*. 2010). The intensity or wavenumber of the peaks slightly shifted in the samples modified with HPC and DBSNa. The reason for this phenomenon is related to the penetration of surfactant in the structure of polymers during the polymerization reaction and change in bonding energies (Cattoz *et al*. 2012; Cho *et al*. 2014).

Considering that the most specific material in RHA is silica (SiO_2), the peaks which represent the behavior of these bonds are important to prove the existence of RHA in the structure (Manique *et al*. 2012). From the results of FTIR, the Si-H stretching, Si-O-Si in plane deformation

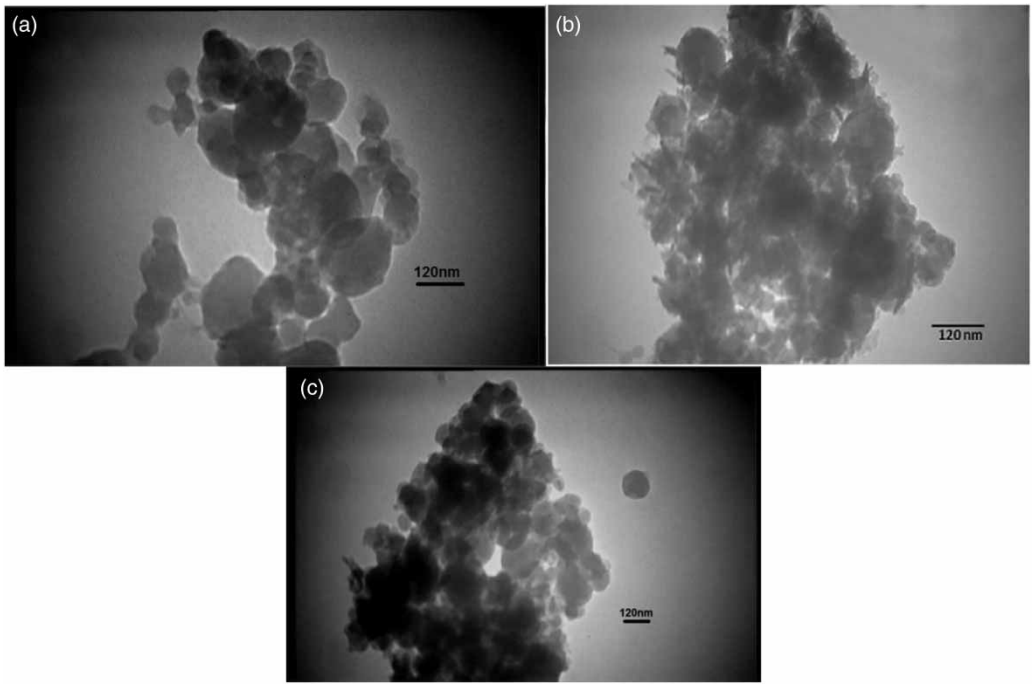

Figure 2 | TEM image of (a) PTh/RHA, (b) PTh/RHA/HPC and (c) PTh/RHA/DBSNa nanocomposite.

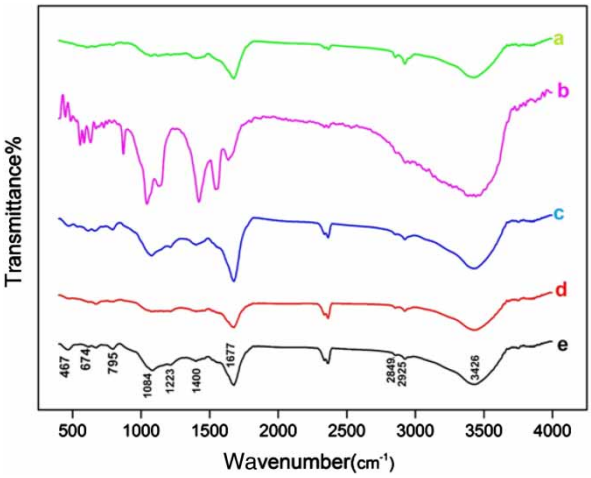

Figure 3 | FTIR spectra of (a) PTh, (b) RHA, (c) PTh/RHA/DBSNa, (d) PTh/RHA/HPC and (e) PTh/RHA.

peak and Si-OH stretching bonds all appear in the FTIR spectra of PTh nanocomposite with RHA with and without surfactants. Existence of surfactant imposed the same effect as RHA on pure PTh, which results in the observed wavenumber shift and peak intensity change.

In order to perform elemental analysis in the structure of RHA and its nanocomposites with PTh, EDS was employed. According to Figure 4(a), Si, O and Na are the most abundant elements in the structure of RHA. The amount of these elements is decreased in the nanocomposite due to the covering of RHA by PTh. It is obvious that the peak related to Si element has the highest value in the EDS analysis of the nanocomposite which belongs to the sulfur group in the structure of PTh.

Pb(II) removal studies

Effect of pH

One of the most important parameters which affects the adsorption of ions on the adsorbent is pH of the solution. The electrical charge on the adsorbent surface and adsorbed ions changes for different pH of solution. In other words, the surface characteristics of adsorbents are highly pH-dependent. At high pH values, negative charges are present on the cell walls, while at low pH values, the overall charge of the cells is positive due to protonation reactions, which prevents the adsorption of positive ions (Brown & Hem 1984; Lataye *et al.* 2006; Pashai Gatabi *et al.* 2016). From the results shown in Figure 5, the optimum pH value for Pb(II) ion adsorption for PTh/RHA-based adsorbents was between 3 and 4 with maximum efficiency of 79%, 91% and 96.58% for

Table 1 | FTIR characterization details of PTh/RHA nanocomposite and surface modified PTh/RHA nanocomposites

Assignments		PTh	RHA	PTh/RHA	PTh/RHA/DBSNa	PTh/RHA/HPC
Si-H	Stretching	–	486	467	486	475
C-H	Out of plane deformation	675	–	674	668	667
C-S-C	Ring deformation	604	–	615	619	617
C-S	Stretching	795	–	795	800	794
Si-O-Si & C-H	In plane deformation	–	1,043	1,084	1,085	1,077
C-O	Stretching	–	1,129	1,223	1,223	1,219
C=C	Stretching ring	1,402	–	1,400	1,401	1,401
C=C	Stretching aromatic (RHA)	–	1,543	1,563	1,556	1,557
C=O & C=C	Stretching & vibration ring	1,668	1,636	1,677	1,678	1,677
C-H	Stretching alkene	2,853	2,935	2,849	2,850	2,857
C-H	Stretching aromatic	2,924	–	2,925	2,924	2,924
O-H & Si-OH	Stretching water of KBr	3,426	3,440	3,426	3,429	3,428

PTh/RHA, PTh/RHA/DBSNa and PTh/RHA/HPC, respectively. In addition, it is evident that among the adsorbents, PTh/RHA/HPC had the highest efficiency. In all samples, the increase in adsorption capacity by increasing pH is due to the presence of H^+ ions in lower pH values which compete with Pb(II) ions for adsorption sites on the adsorbent (Yang *et al.* 2014; Ansari *et al.* 2015). For pH values higher than 6, the Pb(II) ions will precipitate and therefore these pH values were not studied (Xu *et al.* 2011).

Adsorption isotherms

Adsorption equilibrium isotherms are usually used for the determination of the adsorbent capacity for metal ions removal. The most common types are Langmuir and Freundlich, although others are available: Redlich-Peterson, Toth, Sips and Temkin (Miretzky *et al.* 2006). It is important to note that these models do not reflect any mechanisms of sorbate uptake; the equations are just capable of reflecting the experimental data.

The Langmuir model is suitable for monolayer adsorption on a surface, and is expressed as following equation:

$$q_e = \frac{q_m K_L C_e}{1 + K_L C_e} \tag{5}$$

where q_e is the adsorbed Pb(II) concentration at equilibrium (mg/g); C_e is Pb(II) concentration in solution at equilibrium (mg/L); q_m is maximum adsorption capacity (mg/g) and K_L represents the adsorption energy (L/mg).

The Freundlich model is applied on the basis that stronger binding sites are occupied first and is applicable for the adsorbents with heterogeneous structures (Peláez-Cid *et al.* 2013; Iqbal & Khera 2015). The Freundlich equation can be expressed as:

$$q_e = K_F C_e^{1/n_f} \tag{6}$$

where K_F is related to the adsorption capacity (L/mg). The bigger the K_F, the greater the adsorption capacity. In addition, the values of n, which indicate the adsorption driving force, in the range of 1–10, represent good tendency of adsorption (Shahwan & Erten 2004).

The effects of indirect adsorbent/adsorbate interactions on adsorption isotherms and variation of heat of adsorption for all of the molecules in the layer with coverage can be represented by Sips isotherm with the following form:

$$q_e = \frac{q_s (K_s C_e)^{1/n_s}}{1 + (K_s C_e)^{1/n_s}} \tag{7}$$

where K_S is Sips isotherm constant (L/mg) and q_s is the maximum adsorption capacity (mg/g).

Adsorption isotherms of Pb(II) ions on PTh/RHA, PTh/RHA/HPC and PTh/RHA/DBSNa, simulated by the three non-linear isotherm models (Langmuir, Sips and Freundlich), are shown in Figure 6 with all the correlation coefficients and constants listed in Table 2. It can be seen that Freundlich model ($R^2 > 0.99$) gives a better fit compared to Langmuir for both PTh/RHA/HPC

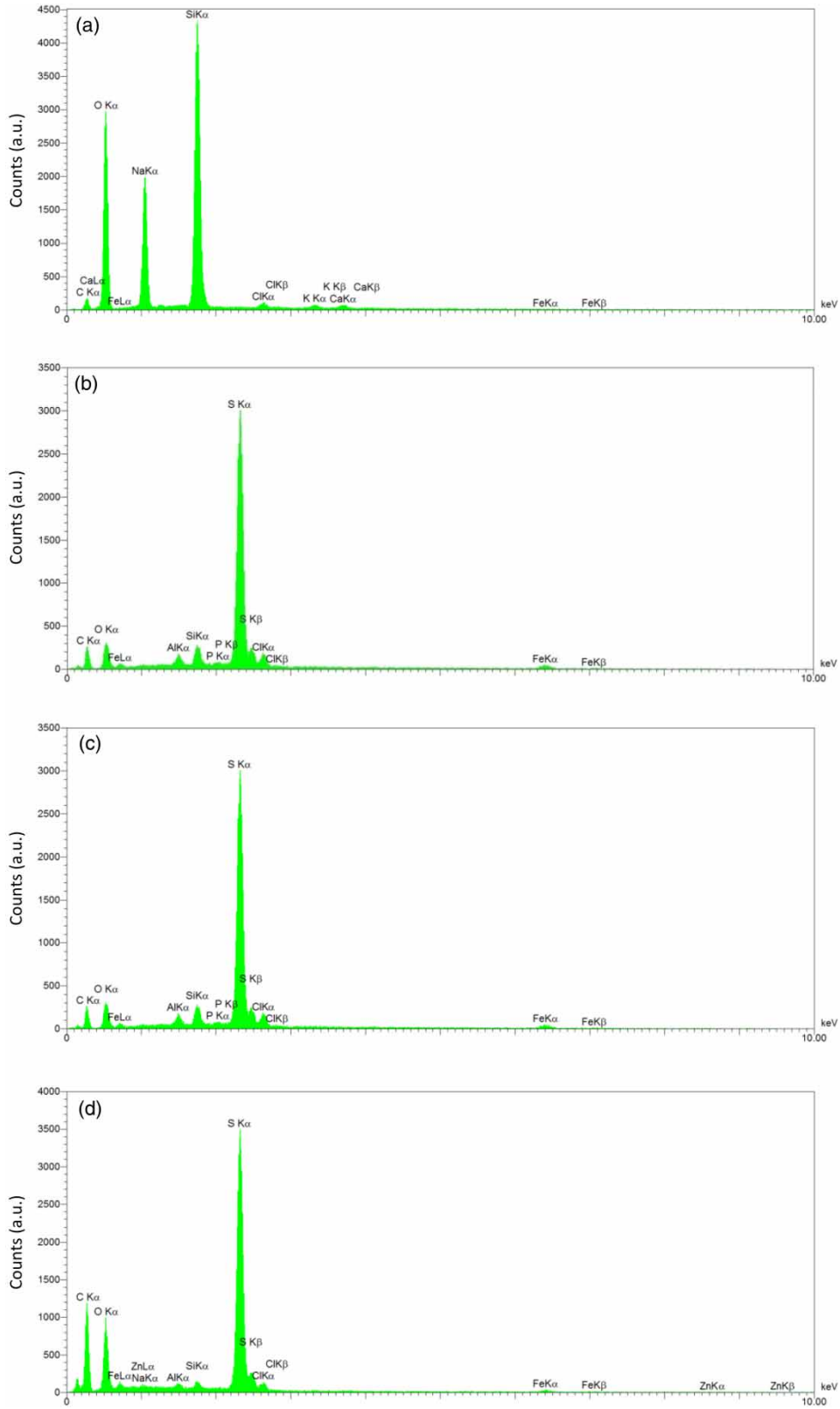

Figure 4 | EDS spectra of (a) RHA, (b) PTh/RHA, (c) PTh/RHA/HPC and (d) PTh/RHA/DBSNa nanocomposite.

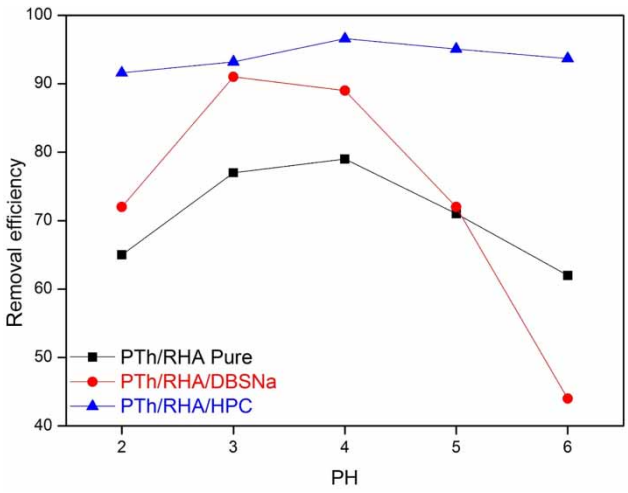

Figure 5 | Effect of pH on the adsorption efficiency and capacity of PTh/RHA, PTh/RHA/HPC and PTh/RHA/DBSNa adsorbents.

($R^2 = 0.990$) and PTh/RHA ($R^2 = 0.995$). On the other hand, adsorption of Pb(II) ions on PTh/RHA/DBSNa was best described by Langmuir isotherm with $R^2 = 0.996$. Considering that the Sips isotherm model is a combination of Langmuir and Freundlich isotherms, it is expected that the adsorption of Pb(II) on PTh/RHA-based adsorbents also correlates with this isotherm. According to the values of correlation coefficients, Sips model had the highest consistency with the experimental data ($R^2 > 0.98$), which represents that multilayer adsorption was performed on adsorbents with heterogeneous sites and different energies of adsorption. The used adsorbents in this study also have different sites (carbon, silica, sulfur etc.); thus, the reason for good correlation of data with this isotherm is logical.

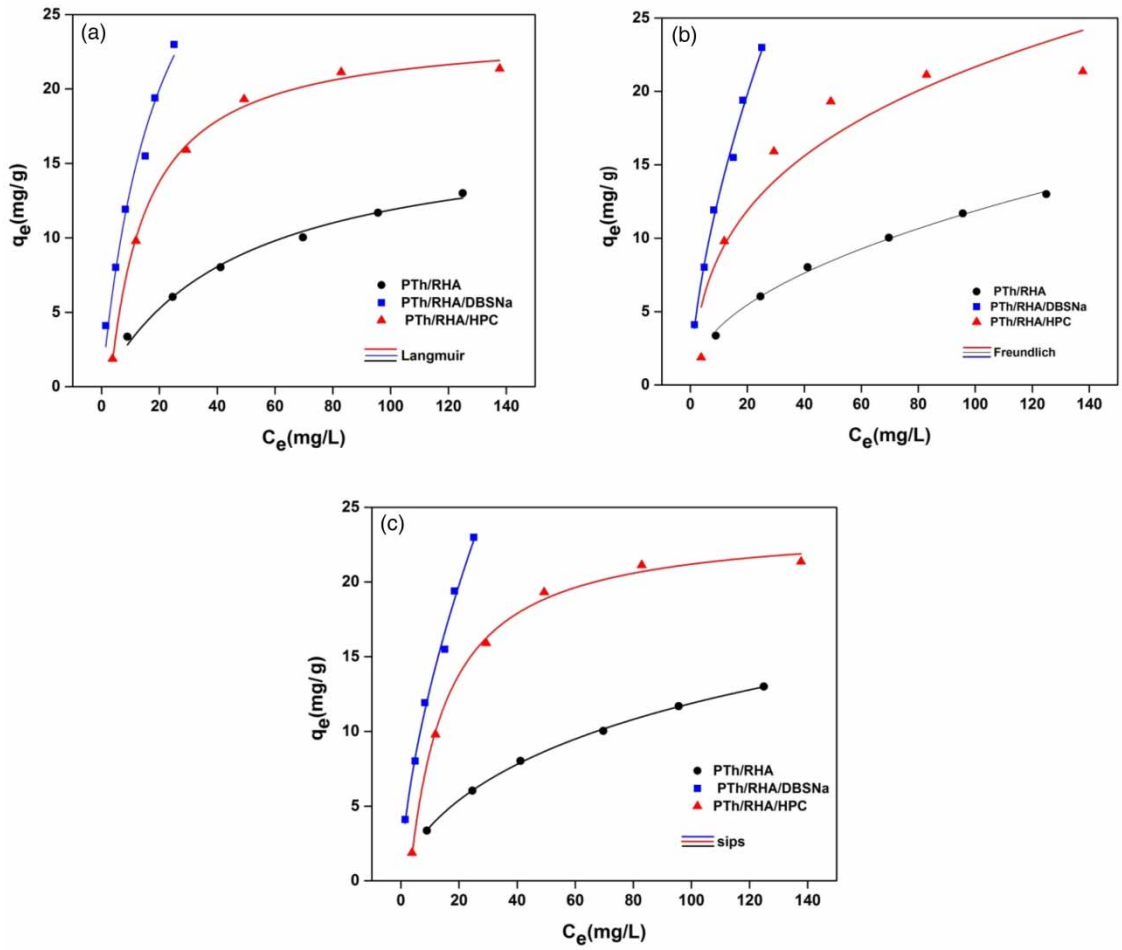

Figure 6 | (a) Langmuir, (b) Freundlich and (c) Sips isotherms non-linear curve fitting on experimental data.

Table 2 | Calculated parameters from fitting the Freundlich, Langmuir and Sips isotherms on experimental data of Pb(II) adsorption on PTh/RHA-based adsorbents

Isotherm parameters	PTh/RHA	PTh/RHA/DBSNa	PTh/RHA/HPC
Langmuir			
K_l (L/mg)	0.022	0.100	0.049
q_m (mg/g)	17.370	13.550	40.290
R^2	0.988	0.996	0.970
Freundlich			
K_f (L/mg)	1.280	3.750	3.050
1/n	0.482	0.261	0.623
R^2	0.995	0.870	0.990
Sips			
q_m (mg/g)	30.429	13.500	2,253.940
K_s (L/mg)	0.028	0.098	0.001
$1/n_s$	0.670	1.011	0.627
R^2	0.999	0.995	0.980

Kinetic studies

The pseudo-first-order model and the pseudo-second-order model were adopted to analyze the adsorption kinetics of Pb(II) on PTh/RHA-based adsorbents. The linear forms of the models are as follows:

$$log(q_e - q_t) = logq_e - \frac{k_1}{2.303}t \quad (8)$$

$$\frac{t}{q_t} = \frac{1}{k_2 q_e^2} + \frac{1}{q_e}t \quad (9)$$

where k_1 and k_2 are the adsorption rate constants for the first and second order kinetic models, respectively.

A plot (Figure 7(a)) of log ($q_e - q_t$) versus t according to the pseudo-first-order kinetic model gives a straight line at the initial 60 min. However, the pseudo-second-order kinetic model (Figure 7(b)) is suitable for 120 min of adsorption process.

The adsorption rate constants (k_1 and k_2) calculated from the slope and the intercept of linear plots are listed in Table 3. The consistency of the experimental q_e with the one calculated from the pseudo-second-order kinetic model illustrates that the adsorption of Pb(II) onto PTh/RHA, PTh/RHA/DBSNa and PTh/RHA/HPC, at initial concentration of 50 mg/L, may be controlled by chemical adsorption (Karaoğlu *et al.* 2010). In addition, higher K_2 values for PTh/RHA/HPC (0.156/min) compared to PTh/RHA and PTh/RHA/DBSNa indicates that Pb(II) ion adsorption on PTh/RHA/HPC takes place with higher rates, requiring shorter time to reach equilibrium.

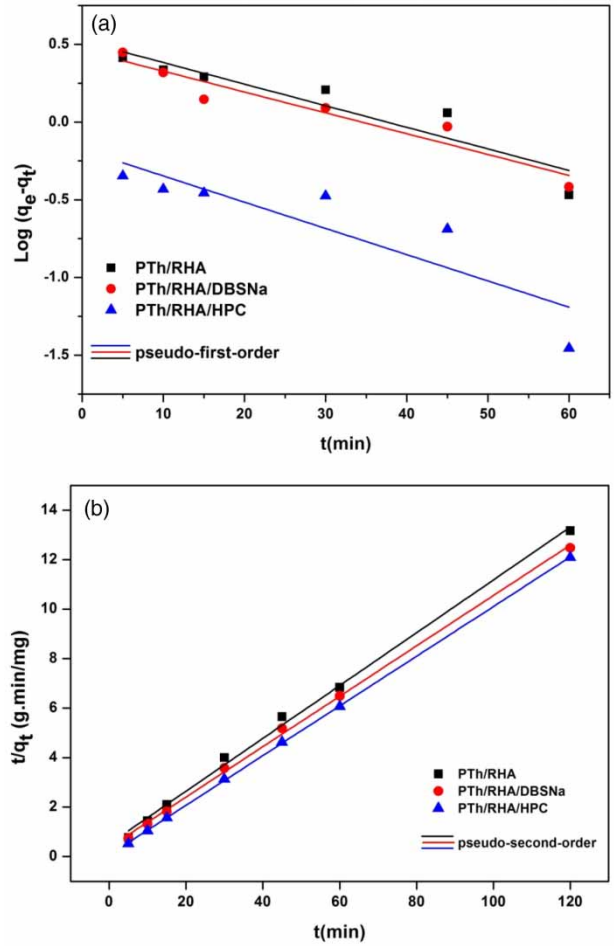

Figure 7 | Kinetic modeling of Pb(II) adsorption on PTh/RHA,PTh/RHA/DBSNa and PTh/RHA/HPC: (a) pseudo-first-order kinetic model and (b) pseudo-second-order kinetic model.

Table 3 | Kinetic model parameters for Pb(II) adsorption on PTh/RHA-based nanoadsorbents

Kinetic models	PTh/RHA	PTh/RHA/DBSNa	PTh/RHA/HPC
Pseudo-first-order			
k_1 (g/min)	0.031	0.0320	0.009
q_e (mg/g)	3.32	1.586	0.443
R^2	0.800	0.860	0.667
Pseudo-second-order			
k_2 (g/mg·min)	0.022	0.027	0.156
q_e (mg/g)	9.367	9.823	10.000
R^2	0.996	0.998	0.999
Experimental data			
q_e (mg/g)	9.107	9.617	9.920

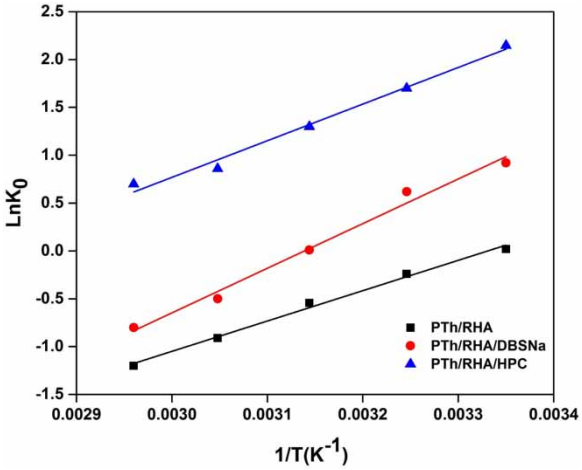

Figure 8 | Van't Hoff plot of Pb(II) adsorption on PTh/RHA-based nanoadsorbents.

Adsorption thermodynamics

Figure 8 and Table 4 illustrate the calculated thermodynamic parameters from Equations (3) and (4). From the results, the negative values of ΔG^0 represent the spontaneous adsorption of Pb(II) on PTh/RHA-based adsorbents. Also the negative ΔH^0 shows the exothermic nature of this adsorption and points that the adsorption is more active at lower temperatures. The negative value of ΔS^0 also shows that the efficiency of adsorption decreased by increasing the temperature of solid and liquid interface (Li *et al.* 2005; Sheela & Nayaka 2012).

Table 4 | Thermodynamic parameters of Pb(II) adsorption on PTh/RHA-based nanoadsorbents

	Thermodynamic parameters			
	Temperature (°K)	ΔG^0 (kJ/mol)	ΔH^0 (kJ/mol)	ΔS^0 (kJ/mol)
PTh/RHA	298	−0.047	− 26.368	− 0.087
	308	−0.614		
	318	1.438		
	328	2.481		
	338	3.372		
PTh/RHA/DBSNa	298	−2.281	− 38.789	− 0.121
	308	−1.587		
	318	−0.748		
	328	1.568		
	338	2.248		
PTh/RHA/HPC	298	−5.316	− 31.825	− 0.089
	308	−4.937		
	318	−2.963		
	328	−2.645		
	338	−2.481		

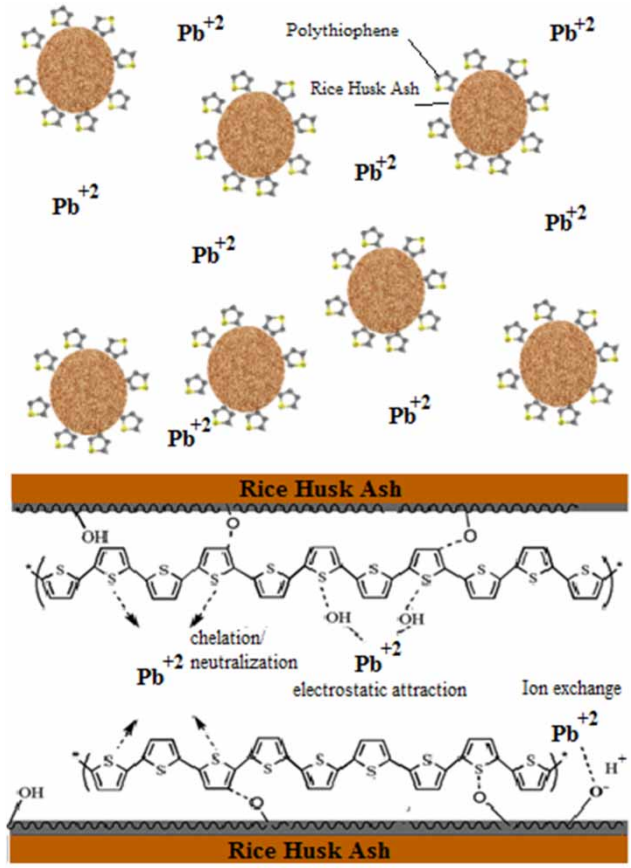

Figure 9 | Schematic of Pb(II) adsorption mechanism on PTh/RHA-based adsorbents.

Adsorption mechanism

The batch adsorption experiments were carried out to investigate the effect of adsorption parameters and the behavior of prepared adsorbents in the removal of Pb(II) ions. Figure 9 indicates a schematic of Pb(II) adsorption mechanism on PTh/RHA-based adsorbents. There are two different mechanisms in the adsorption of Pb(II) on PTh/RHA-based adsorbents: (i) physical adsorption on the surface of PTh or in the pores of the adsorbent and (ii) chemical adsorption through interactions of PTh molecules with Pb(II) ions. RHA has a porous structure that leads to high specific surface area of the adsorbent. Therefore, Pb(II) ions can penetrate through the adsorbent porosity and adsorb on the surface of RHA or PTh. On the other hand, another probable adsorption mechanism occurring on the surface of PTh is via electrostatic interaction of OH groups, bonded to sulfur on the structure of PTh, and Pb(II) ions and chelation or neutralization interactions of sulfur groups and Pb(II) (Kannan & Sundaram 2001; Alizadeh *et al.* 2016).

CONCLUSION

The surface modified PTh/RHA adsorbents were synthesized in the presence of HPC and DBSNa as surfactant to be used for adsorption of Pb(II) ion from waste water. The nanocomposite adsorbents were prepared by coating the RHA substrate with thiophene using the chemical oxidative polymerization method and its capability to remove lead ions from aqueous solution was studied. The characteristics of PTh/RHA-based nanocomposite adsorbents, such as morphology and molecular structure were also investigated. It was found that RHA nanoparticles had an important effect on particle size distribution and morphology of the resulting products. The FTIR spectra confirmed the presence of PTh in the nanocomposite structure. The results indicated that the intensities of peaks are dependent on the presence of silicon dioxide and HPC or DBSNa.

Batch adsorption experiments were performed for lead ion removal from aqueous solution. The adsorption characteristics were tested at different pH values, contact times, and initial concentrations of Pb(II). The results can be summarized as follows:

- The percentage removal of lead ions increases with decreasing pH of the solution and an optimum value of approximately 3–4 was achieved.
- Among the synthesized PTh/RHA-based adsorbents, PTh/RHA/HPC had the highest efficiency (96.58%) at $pH = 4$.
- The Freundlich adsorption isotherm model was better fitted with experimental data for both PTh/RHA and PTh/RHA/HPC in comparison to Langmuir adsorption isotherm models.
- The non-linear Sips isotherm model was best to predict the adsorption of Pb(II) on PTh/RHA/HPC, PTh/RHA/DBSNa and PTh/RHA nanocomposite with high correlation coefficients ($R^2 > 0.98$) obtained at a higher confidence level.
- The pseudo-first-order model and the pseudo-second-order model were adopted to analyze the adsorption kinetics of Pb(II) on PTh/RHA/HPC.
- The consistency of the experimental q_e with adsorption capacities calculated from the pseudo-second-order kinetic model illustrates that the adsorption of Pb(II) onto PTh/RHA-based adsorbents, at initial concentration of 50 mg/L, was mainly controlled by chemical adsorption.

On the basis of these results, surface modified PTh/RHA nanocomposites were found to be appropriate for the removal of Pb(II) from the aqueous solution.

REFERENCES

Ali, I. & Gupta, V. 2006 Advances in water treatment by adsorption technology. *Nature Protocols* **1** (6), 2661–2667.

Alizadeh, B., Ghorbani, M. & Salehi, M. A. 2016 Application of polyrhodanine modified multi-walled carbon nanotubes for high efficiency removal of Pb(II) from aqueous solution. *Journal of Molecular Liquids* **220**, 142–149.

Ansari, R., Tehrani, M. S. & Keivani, M. B. 2013 Application of polythiophene–sawdust nano-biocomposite for basic dye removal using a continuous system. *Journal of Wood Chemistry and Technology* **33** (1), 19–32.

Ansari, M. O., Khan, M. M., Ansari, S. A. & Cho, M. H. 2015 Polythiophene nanocomposites for photodegradation applications: past, present and future. *Journal of Saudi Chemical Society* **19** (5), 494–504.

Barakat, M. 2011 New trends in removing heavy metals from industrial wastewater. *Arabian Journal of Chemistry* **4** (4), 361–377.

Bradl, H. 2005 *Heavy Metals in the Environment: Origin, Interaction and Remediation.* Academic Press, Amsterdam.

Brown, D. W. & Hem, J. D. 1984 *Development of a Model to Predict the Adsorption of Lead from Solution on a Natural Streambed Sediment*, US Geological Survey Water-Supply Paper 2187, USGPO, Washington.

Cattoz, B., Cosgrove, T., Crossman, M. & Prescott, S. W. 2012 Surfactant-mediated desorption of polymer from the nanoparticle interface. *Langmuir* **28** (5), 2485–2492.

Cho, J. M., Kwak, S.-W., Aqoma, H., Kim, J. W., Shin, W. S., Moon, S.-J., Jang, S.-Y. & Jo, J. 2014 Effects of ultraviolet–ozone treatment on organic-stabilized ZnO nanoparticle-based electron transporting layers in inverted polymer solar cells. *Organic Electronics* **15** (9), 1942–1950.

Dylla-Spears, R., Feit, M., Miller, P. E., Steele, W. A., Suratwala, T. I. & Wong, L. L. 2015 Method for preventing agglomeration of charged colloids without loss of surface activity. US Patent 20,150,275,048.

Eisazadeh, H. 2007 Removal of chromium from waste water using polyaniline. *Journal of Applied Polymer Science* **104** (3), 1964–1967.

Falcão, E. H. & de Azevêdo, W. M. 2002 Polyaniline-poly (vinyl alcohol) composite as an optical recording material. *Synthetic Metals* **128** (2), 149–154.

Ghorbani, M. & Eisazadeh, H. 2012 Fixed bed column study for Zn, Cu, Fe and Mn removal from wastewater using nanometer size polypyrrole coated on rice husk ash. *Synthetic Metals* **162** (15), 1429–1433.

Ghorbani, M., Eisazadeh, H. & Katal, R. 2010 Fixed-bed column study of the removal of anions and heavy metals from cotton textile waste water by using polyaniline and its nanocomposite containing nanometer-size Fe_3O_4. *Journal of Vinyl and Additive Technology* **16** (3), 217–221.

Ho, Y.-S. 2003 Removal of copper ions from aqueous solution by tree fern. *Water Research* **37** (10), 2323–2330.

Iqbal, M. & Khera, R. A. 2015 Adsorption of copper and lead in single and binary metal system onto *Fumaria indica* biomass. *Chemistry International* **1** (3), 157b–163b.

Kannan, N. & Sundaram, M. M. 2001 Kinetics and mechanism of removal of methylene blue by adsorption on various carbons –a comparative study. *Dyes and Pigments* **51** (1), 25–40.

Karaoğlu, M. H., Doğan, M. & Alkan, M. 2010 Kinetic analysis of reactive blue 221 adsorption on kaolinite. *Desalination* **256** (1), 154–165.

Khambhaty, Y., Mody, K., Basha, S. & Jha, B. 2009 Kinetics, equilibrium and thermodynamic studies on biosorption of hexavalent chromium by dead fungal biomass of marine *Aspergillus niger*. *Chemical Engineering Journal* **145** (3), 489–495.

Lataye, D. H., Mishra, I. M. & Mall, I. D. 2006 Removal of pyridine from aqueous solution by adsorption on bagasse fly ash. *Industrial & Engineering Chemistry Research* **45** (11), 3934–3943.

Lee, K. P., Arnot, T. C. & Mattia, D. 2011 A review of reverse osmosis membrane materials for desalination – development to date and future potential. *Journal of Membrane Science* **370** (1), 1–22.

Li, N., Lee, J. & Ong, L. 1992 A polyaniline and Nafion® composite film as a rechargeable battery. *Journal of Applied Electrochemistry* **22** (6), 512–516.

Li, Y.-H., Di, Z., Ding, J., Wu, D., Luan, Z. & Zhu, Y. 2005 Adsorption thermodynamic, kinetic and desorption studies of Pb^{2+} on carbon nanotubes. *Water Research* **39** (4), 605–609.

Li, X., Li, C., Chen, J., Li, C. & Sun, C. 2008 Polythiophene as a novel fiber coating for solid-phase microextraction. *Journal of Chromatography A* **1198**, 7–13.

Liu, R. & Liu, Z. 2009 Polythiophene: synthesis in aqueous medium and controllable morphology. *Chinese Science Bulletin* **54** (12), 2028–2032.

MacDiarmid, A. G. & Epstein, A. J. 1995 Secondary doping in polyaniline. *Synthetic Metals* **69** (1), 85–92.

Manique, M. C., Faccini, C. S., Onorevoli, B., Benvenutti, E. V. & Caramão, E. B. 2012 Rice husk ash as an adsorbent for purifying biodiesel from waste frying oil. *Fuel* **92** (1), 56–61.

Matsuguchi, M., Io, J., Sugiyama, G. & Sakai, Y. 2002 Effect of NH_3 gas on the electrical conductivity of polyaniline blend films. *Synthetic Metals* **128** (1), 15–19.

Miretzky, P. & Cirelli, A. F. 2009 Hg (II) removal from water by chitosan and chitosan derivatives: a review. *Journal of Hazardous Materials* **167** (1), 10–23.

Miretzky, P., Saralegui, A. & Cirelli, A. F. 2006 Simultaneous heavy metal removal mechanism by dead macrophytes. *Chemosphere* **62** (2), 247–254.

Ohtani, A., Abe, M., Ezoe, M., Doi, T., Miyata, T. & Miyake, A. 1993 Synthesis and properties of high-molecular-weight soluble polyaniline and its application to the 4MB-capacity barium ferrite floppy disk's antistatic coating. *Synthetic Metals* **57** (1), 3696–3701.

Pashai Gatabi, M., Milani Moghaddam, H. & Ghorbani, M. 2016 Point of zero charge of maghemite decorated multiwalled carbon nanotubes fabricated by chemical precipitation method. *Journal of Molecular Liquids* **216**, 117–125.

Peláez-Cid, A., Velazquez-Ugalde, I., Herrera-González, A. & García-Serrano, J. 2013 Textile dyes removal from aqueous solution using *Opuntia ficus-indica* fruit waste as adsorbent and its characterization. *Journal of Environmental Management* **130**, 90–97.

Ren, X., Chen, C., Nagatsu, M. & Wang, X. 2011 Carbon nanotubes as adsorbents in environmental pollution management: a review. *Chemical Engineering Journal* **170** (2), 395–410.

Rosthauser, J. W., Meckel, W. & Rasshofer, W. 1991 Emulsion reaction, surfactant to prevent agglomeration, pigment incorporated during polymerization. US Patent 4,985,490.

Shahwan, T. & Erten, H. 2004 Temperature effects in barium sorption on natural kaolinite and chlorite-illite clays. *Journal of Radioanalytical and Nuclear Chemistry* **260** (1), 43–48.

Sheela, T. & Nayaka, Y. A. 2012 Kinetics and thermodynamics of cadmium and lead ions adsorption on NiO nanoparticles. *Chemical Engineering Journal* **191**, 123–131.

Srivastava, V. C., Mall, I. D. & Mishra, I. M. 2006 Characterization of mesoporous rice husk ash (RHA) and adsorption kinetics of metal ions from aqueous solution onto RHA. *Journal of Hazardous Materials* **134** (1), 257–267.

Theron, J., Walker, J. & Cloete, T. 2008 Nanotechnology and water treatment: applications and emerging opportunities. *Critical Reviews in Microbiology* **34** (1), 43–69.

Vatani, Z. & Eisazadeh, H. 2013 Application of polythiophene nanocomposite coated on polystyrene and poly(vinyl chloride) for removal of Pb(II) from aqueous solution. *Polymer-Plastics Technology and Engineering* **52** (15), 1621–1625.

Xu, S. H., Li, S. Y., Wei, Y. X., Zhang, L. & Xu, F. 2010 Improving the photocatalytic performance of conducting polymer polythiophene sensitized TiO_2 nanoparticles under sunlight irradiation. *Reaction Kinetics, Mechanisms and Catalysis* **101** (1), 237–249.

Xu, M., Zhang, Y., Zhang, Z., Shen, Y., Zhao, M. & Pan, G. 2011 Study on the adsorption of Ca^{2+}, Cd^{2+} and Pb^{2+} by magnetic Fe_3O_4 yeast treated with EDTA dianhydride. *Chemical Engineering Journal* **168** (2), 737–745.

Yang, Z., Zhang, W., Wang, T. & Li, J. 2014 Improved thiophene solution selectivity by Cu^{2+}, Pb^{2+} and Mn^{2+} ions in pervaporative poly[bis(p-methyl phenyl) phosphazene] desulfurization membrane. *Journal of Membrane Science* **454**, 463–469.

Yaşar, M., Deligöz, H. & Güçlü, G. 2011 Removal of indigo carmine and Pb(II) ion from aqueous solution by polyaniline. *Polymer-Plastics Technology and Engineering* **50** (9), 882–892.

First received 16 December 2016; accepted in revised form 21 February 2017. Available online 13 March 2017